A Journal of the Gesellschaft Deutscher Chemiker

Angewandte International Edition Chemie

GDCh

www.angewandte.org

Accepted Article

Title: Secondary Structure-Driven Self-Assembly of Reactive Polypept(o)ides: Controlling Size, Shape and Function of Core Cross-Linked Nanostructures

Authors: Kristina Klinker, Olga Schäfer, David Huesmann, Tobias Bauer, Leon Capelôa, Lydia Braun, Natascha Stergiou, Meike Schinnerer, Anjaneyulu Dirisala, Kanjiro Miyata, Kensuke Osada, Horacio Cabral, Kazunori Kataoka, and Matthias Barz

To be cited as: *Angew. Chem. Int. Ed.* 10.1002/anie.201702624
Angew. Chem. 10.1002/ange.201702624

Link to VoR: http://dx.doi.org/10.1002/anie.201702624
http://dx.doi.org/10.1002/ange.201702624

WILEY-VCH

10.1002/anie.201702624

WILEY-VCH

Secondary Structure-Driven Self-Assembly of Reactive Polypept(o)ides: Controlling Size, Shape and Function of Core Cross-Linked Nanostructures

Kristina Klinker[+], Olga Schäfer[+], David Huesmann, Tobias Bauer, Leon Capelôa, Lydia Braun, Natascha Stergiou, Meike Schinnerer, Anjaneyulu Dirisala, Kanjiro Miyata, Kensuke Osada, Horacio Cabral, Kazunori Kataoka, Matthias Barz*

Controlling the self-assembly of block copolymers in solution offers a versatile and powerful method to create nanometer-sized particles with defined and controllable geometry, size, and functionality.[1–4] Size, shape and internal structure of nano-sized objects obtained by aggregation of amphiphilic coil-coil block copolymers in a block selective solvent in thermodynamic equilibrium is mainly dictated by the ratio of the volume fraction between the solvophilic and solvophobic block.[5] The self-assembly of rod-coil block copolymers is additionally driven by aggregation of the rod segment and the formation of orientational order, which may lead to morphologies different from those obtained from typical coil-coil polymers.[6–9] In crystallization-driven self-assembly, different types of polymers have been described as rod segments throughout the literature, among them polyferrocenylsilane (PFS) block copolymers with poly(dimethyl-siloxane) (PDMS), polyisoprene (PI) and poly(lactic acid).[10–12] In contrast to this type of organization, anisotropic nanomaterials can also be obtained by controlled aggregation of peptide amphiphiles (PAs), a concept well-established in supramolecular chemistry.[7,13–15] In these systems, self-assembly is predominantly driven by secondary structure formation of the peptide segment. It is noteworthy that β-sheet-driven polypeptide self-assembly is so far mostly limited to sequence-defined peptides.[16–19] Approaches using ring-opening polymerization of α-amino acid *N*-carboxyanhydrides (NCAs) to create the peptidic rod-like segment have also been used to stabilize micellar aggregates *in vivo*,[20] to induce aggregation of oligomers or to create smart materials that can be switched from rod-coil to coil-coil using external stimuli such as temperature, pH and chaotropic agents.[21,22] However, approaches utilizing synthetic polypeptides derived by NCA polymerization are mostly restricted to α-helical motifs since synthesis of β-sheet forming polymers is not trivial to achieve.[23] Therefore, directing morphology of polymeric micelles by β-sheet formation of the hydrophobic core-forming synthetic polypeptide has not yet been realized.

Cysteine is a particularly interesting amino acid because of its thiol side chain for potential bio-reversible modification and its propensity to adopt a β-sheet conformation in solution.[24] Our group has recently introduced *S*-alkylsulfonyl-protected cysteine NCAs,[25] which enable controlled ring-opening polymerization, yielding average chain lengths up to 30 repeat units of well-defined polymers with intrinsic anti-paralell ß-sheet

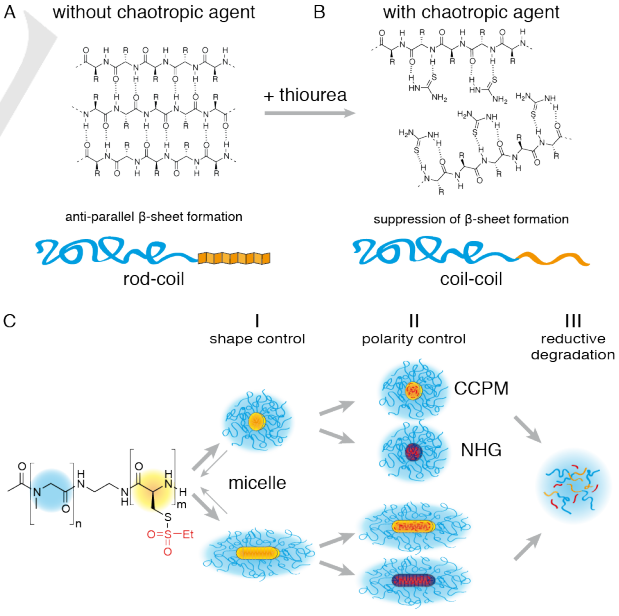

Figure 1. A) Schematic representation of anti-paralell ß-sheet formation and B) suppressed secondary structures by chaotropic agents (e.g., thiourea) C) Illustration of the proposed platform featuring the following phases: (I) self-assembly of amphiphilic $PSar_n$-*b*-$PCys(SO_2Et)_m$ block copolymers into different micellar morphologies directed by secondary structure alignment, (II) subsequent core cross-linking by disulfides of choice, yielding core cross-linked polymeric micelles (CCPM) or nanonydrogels (NHG) and (III) disintegration of the system upon a reductive stimulus.

[*] K. Klinker[+] O. Schäfer[+] Dr. D. Huesmann, T. Bauer, L. Capelôa, L. Braun, M. Schinnerer, Dr. M. Barz
Institute of Organic Chemistry
Johannes Gutenberg University Mainz
Duesbergweg 10-14, 55128 Mainz, Germany
E-mail: barz@uni-mainz.de
K. Klinker[+]
Graduate School Materials Science in Mainz,
Staudinger Weg 9, 55128 Mainz, Germany
N. Stergiou
University Medical Center-Institute of Immunology
Johannes Gutenberg University Mainz
Langenbeckstrasse 1, Geb. 708, 55101 Mainz, Germany
Dr. A. Dirisala, Prof. Dr. K. Kataoka
Innovation Center of NanoMedicine
KAWASAKI Institute of Industrial Promotion
3-25-14, Tonomachi, Kawasaki-ku, Kawasaki 210-0821
Prof. Dr. K. Miyata
Department of Materials Engineering
Graduate School of Engineering, The University of Tokyo
7-3-1 Hongo, Bunkyo-ku, Tokyo 113–8656, Japan
Prof. Dr. K. Osada, Prof. Dr. H. Cabral,
Department of Bioengineering
Graduate School of Engineering, The University of Tokyo
7-3-1 Hongo, Bunkyo-ku, Tokyo 113–8656, Japan
Prof. Dr. K. Kataoka
Policy Alternatives Research Institute, The University of Tokyo
7-3-1 Hongo, Bunkyo-ku, Tokyo 113–8656, Japan

[+] These authors contributed equally to this work.

Supporting information for this article is available under:

conformation.[26] Employed as a building block in polypept(o)ides, a unique material can be obtained that combines functionality, stimuli-responsiveness, and secondary structure formation of polypeptides with the stealth-like properties of the coil-forming polypeptoid polysarcosine (PSar).[27] Keeping in mind that secondary structure of proteins can be denatured by different external stimuli,[28] the self-assembly of these block copolypept(o)ides should be controllable by switching from rod-coil block copolymers (intact β-sheet conformation, Figure 1A) to coil-coil polymers by a chaotropic agent (disturbed β-sheet conformation, Figure 1B).

Apart from constituting the driving force for self-assembly (Figure 1CI), the *S*-alkyl sulfonyl cysteine block remains highly reactive towards thiols after polymerization.[29] This chemoselective reactivity enables core cross-linking by asymmetric disulfides (Figure 1CII), which seems suitable to preserve the formed nanoparticle morphologies. $PSar_n$-*b*-$PCys(SO_2Et)_m$ block copolymers can be obtained by NCA polymerization using a bifunctional initiator as reported previously (Scheme S1).[30] Block copolymers with differing block length ratios and total block lengths were successfully prepared with dispersity indices (Đ) between 1.2 - 1.4 (Table S1 and Figure S1). Self-assembly of $PSar_n$-*b*-$PCys(SO_2Et)_m$ block copolymers was investigated methodically by varying two major factors contributing to the overall morphology: the composition of the amphiphile as well as intact or suppressed secondary structure by addition of the chaotropic agent thiourea (TU). The percentage of the hydrophobic cysteine block was kept at 15 wt.% (**P1** X_n/X_m = 407:28, **P2** X_n/X_m = 265:17, determined by ^{1}H NMR), and 30 wt.% (**P3** X_n/X_m 97:15, determined by ^{1}H NMR), respectively. To obtain well-defined micelles, block copolymers were first dissolved in *N*,*N*-dimethylacetamide (DMAc), aggregated in the presence of 20 vol.% 1 mM acetate buffer (Figure S2) and subsequently dialyzed against 1mM acetate buffer to allow the formation of thermodynamically favored structures. For ß-sheet suppression (Figure 1C II), 1 M TU in DMAc and 10 mM in buffer was used. Upon solvent exchange, micelles were core cross-linked by disulfides to stabilize the formed aggregates (triethylenetetramine α,ω-di(cysteine)diamide **c2** was used throughout Figure 2 yielding nanohydrogels, see also Table S2). As obtained morphologies were fixated by cross-linking, size distributions remained fully preserved (Figure 3BI), thus enabling detailed characterization of the particles using dynamic light scattering (DLS), circular dichroism (CD), transmission electron microscopy (TEM) and atomic force microscopy (AFM).

As determined by cumulant analysis of DLS, **P1** formed structures with D_h = 77 nm (**1**) in the absence of TU and considerably smaller structures with D_h = 51 nm (**2**) in presence of TU (Figure 2AII, Table 1). From a theoretical point of view, block copolymers with 15 wt.% hydrophobic block are expected to form spherical micelles.[5] As briefly outlined above, the self-assembly behavior of rod-coil polymers differs considerably from that of coil-coil polymers. In the case of ß-sheet rods, intermolecular interactions between rod chains dominate and an enhanced packing of crystallizing chains can lead to the formation of form-anisotropic /elongated objects. Moreover, ß-sheets tend to arrange in twisted structures[31] also typical for natural peptides, e.g. ß-sheet barrels (Figure 2AI).[32] Coil-coil

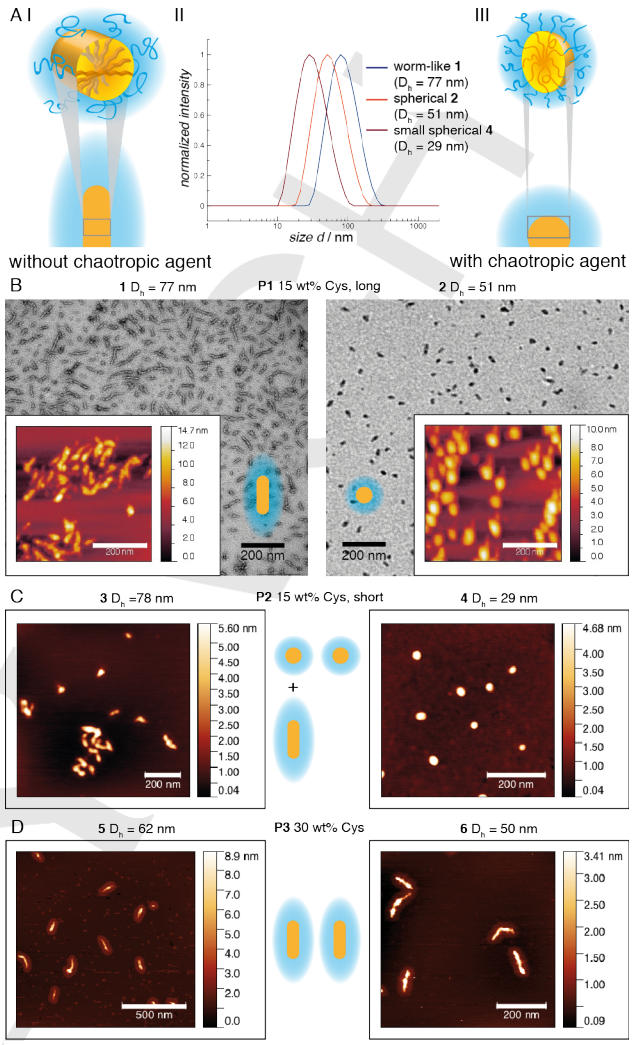

Figure 2. AI) Illustrated core framework of worm-like particles with twisted ß-sheets in the absence of a chaotropic agent. (II) Size range of the obtained core cross-linked nanohydrogels **1**,**2**, and **4** (DLS). (III) Illustrated core framework of spherical particles with interwined polymer chains in random coil conformation due to the presence of a chaotropic agent. B) Shape control of nanohydrogels **1** and **2** (visualized by AFM/TEM) modulated by presence or absence of secondary structure stabilization (from **P1**, 15 wt.% of hydrophobic segment). C) Nanohydrogels from a shorter block copolymer (**P2**, 15 wt.%) exhibit either a mixed morphology in the presence of secondary structures **3** or small-scale spheres **4** (AFM) D) Worm-like nanohydrogels **5** and **6** (AFM) obtained independently from secondary structure stabilization due to a higher weight percentage of the hydrophobic segment of **P3** (30 wt.%).

polymers on the other hand favor rounded interfaces to minimize contact between the less soluble block and the solvent (Figure 2AIII). TEM and AFM were subsequently used to elucidate the morphology of core cross-linked micellar aggregates (Figure 2B and S3). TEM images were stained using uranyl acetate to visualize the polycysteine core,[33] whereas AFM shows the dimensions of the whole particle. Both methods demonstrate the formation of worm-like structures **1** in the rod-coil case (absence of TU) and of spherical micelles **2** in the coil-coil case (presence of TU). The larger D_h of **1** observed in DLS can thus be explained by a one-dimensional growth of twisted anti-parallel ß-

sheet alignments into worm-like micelles. The retained internal ß-sheet structure was further confirmed using CD before and after core cross-linking and purification (Figure S4). Worm-like micelles show a negative Cotton effect at approx. 220 nm, confirming the presence of ß-sheets throughout the particle preparation. Reliable CD data of micelles in the presence of thiourea could not be obtained due to high UV-absorbance of thiourea at relevant concentrations (1 M - 10 mM). Polymer **P2** with the same block-to-block ratio (15 wt.%), but decreased total chain length leads to the formation of a mixture of spherical and worm-like micelles **3** in the absence of TU and small spherical micelles **4** (D_h = 29 nm, Figure 2AII, C and S5) in the presence of TU. This coexistence of morphologies most likely originates from the fact that synthetic block copolymers bear a certain polydispersity, indicating that not all polymer chain have attained the critical length to successfully participate in β-sheet alignments necessary to form exclusively elongated structures. Hence multi-angle DLS revealed an angle-dependent scattering behavior of **3** indicating non-spherical and/or polydisperse samples with a μ_2 of 0.17, whereas **4** showed no angular dependency typical for spherical and uniform particles with a μ_2 of 0.06 indicating low polydispersity (Figure S6). Increasing the percentage of the hydrophobic block to 30 wt.% in polymer **P3** resulted in the formation of worm-like micelles **5** and **6** in both the presence and the absence of thiourea, only differing slightly in hydrodynamic diameter (D_h = 62 nm and 50 nm, respectively, Figure 2D, S5 and S7). This behavior was anticipated for coil-coil polymers with 30 wt.% of the hydrophobic block.[5] Our findings underline the fact that β-sheet formation of the polycysteine block in block copolypept(o)ides substantially influences self-assembly behavior, since it forms a rigid rod segment by intermolecular interactions that can be transformed into coil conformation by the chaotropic agent thiourea. Consequently, a PSar$_n$-*b*-PCys(SO$_2$Et)$_m$ block copolymer with a hydrophobic ratio known to form spherical micelles combined with a certain critical total length will form elongated structures if undisturbed (rod-coil) and spherical structures when transformed into a coil-coil polymer in the presence of TU.

Table 1. Particle characterization of core cross-linked polymeric micelles (CCPM) and nanohydrogels (NHG).

particle	polymer	thiourea	morphology	crosslinker
NHG **1**	**P1**	-	worm-like	cationic (**c2**)
NHG **2**	**P1**	+	spherical	cationic (**c2**)
NHG **3**	**P2**	-	mixed	cationic (**c2**)
NHG **4**	**P2**	+	spherical	cationic (**c2**)
NHG **5**	**P3**	-	worm-like	cationic (**c2**)
NHG **6**	**P3**	+	worm-like	cationic (**c2**)
CCPM **8**	**P2**	+	spherical	hydrophobic (**c1**)
CCPM **10**	**P2**	+	spherical	hydrophobic (**c1**)
CCPM **11**	**P1**	-	worm-like	cationic (**c2**)

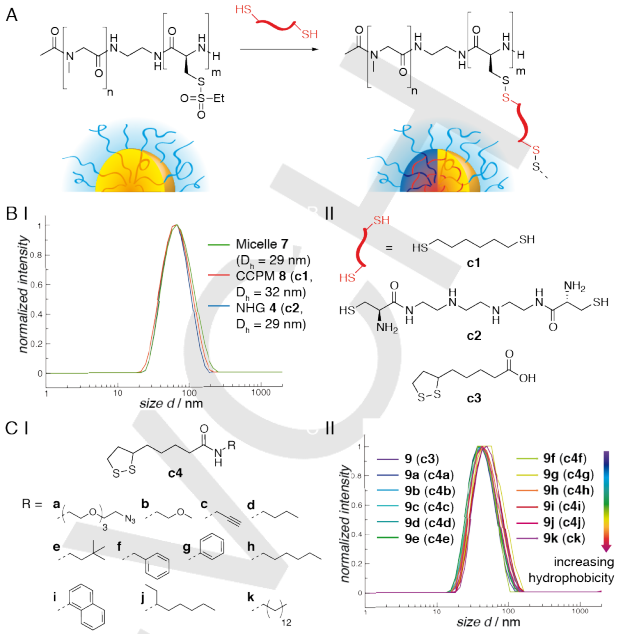

Figure 3. A) Cross-linking of self-assembled nanostructures using the thiol-reactivity of the *S*-ethylsulfonyl group with various dithiols and thus introducing bio-reversible disulfide bonds in cross-linked polymeric micelles (CCPM, yellow core) and nynohydrogels (NHG, blue core). BI) An identical particle size is retained throughout the use of various cross-linkers, (II) while core functionality is changed. CI) Adjusting core polarity of CCPMs with lipoic acid-derived cross-linkers of varying side chains, (II) without affecting particle size.

In addition to morphology control and covalent core cross-linking, the *S*-alkylsulfonyl protective group in PSar$_n$-*b*-PCys(SO$_2$Et)$_m$ block copolymers is particular attractive for the construction of drug delivery systems. This approach can be not only used to incorporate functionality into the core of micelles, but leads to bio-reversible disulfide bonds (Figure 3A and S8). Disulfide cross-linked micelles and polyplexes are known to be stable in blood (10 µM glutathione (GSH)) but are rapidly cleaved inside cells (10 mM GSH).[34,35] Therefore, this type of cross-linking appears ideal to stabilize nanoparticles while they are in circulation, but makes them responsive to a change in redox potential once they enter cells in order to disintegrate and release their cargo specifically.[36] In contrast to the disulfide cross-linking frequently reported in literature, e.g. oxidation in the presence of oxygen[37] or DMSO,[38] the cross-linking reaction of CysSO$_2$Et is thiol-selective, proceeds rapidly, and yields asymmetric disulfides in aqueous solution.[26,29] Having established that core cross-linking does not alter the size distribution of micelles at optimized cross-linking conditions (Figure 3BI, Table S2), it seems highly interesting to investigate, if the adjustment or even the inversion of the core-polarity is possible. In this case, the desired function of the carrier system can be introduced in one single step by the cross-linker itself, allowing for rapid production of nanoparticle libraries from one precursor micelle. While hydrophobic cross-linkers (e.g., hexanedithiol **c1**) form core cross-linked polymeric micelles (CCPMs), cationic cross-linkers (e.g., triethylenetetramine α,ω-di(cysteine)diamide **c2**) invert core polarity and thus lead to the

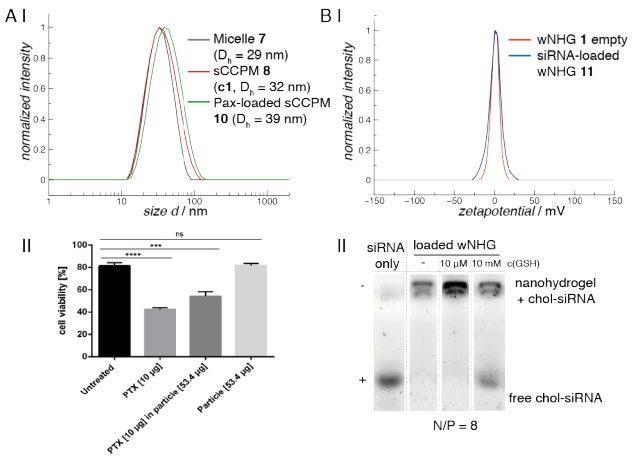

Figure 4: A) Core cross-linked polymeric micelle **8** with cross-linker **c1** loaded with PTX **10** (I) showing uniform micelles prior and after loading as well as (II) pronounced efficacy *in vitro* on TD47 cells. B) Cationic nahohydrogel with cross-linker **c2** prior (**1**) and after complexation of siRNA (**11**) (I) exhibits a near neutral ζ-potentials and (II) enabling stimuli-responsive release at intracellular glutathione levels (10mM).

formation of cationic nanohydrogels (NHGs) (Figure 3BII). Since both structures are derived from polypept(o)ides, we define them as core cross-linked PeptoMicelle and NanoPeptoGel. Successful core cross-linking was verified by gel permeation chromatography in hexafluoro-2-propanol (HFIP), which is a good solvent for both blocks (Figure S9). With core cross-linked polymeric micelles and nanohydrogels as the core polarity extremes, a library of lipoic acid-based cross-linkers **c4a-k** was synthesized to fine-tune core polarity (Figure 3CI, Table S3). In addition to simply altering polarity, residues R of the cross-linker **c4** can readily be adjusted to match, for example, a certain cargo, to covalently attach drugs or imaging probes.[39,40] As shown earlier, the cross-linking reaction (for **c3** and **c4a-k** after equimolar reduction with tris(2-carboxyethyl)phosphine (TCEP), Scheme S2) is independent of the cross-linker's chemical nature and results in particles **9a-g** with comparable size distributions (Figure 3CII, Table S2). These findings underline that nanostructure formation is completely separated from chemical functionality in this approach, which is a very desirable characteristic in a new material.

Furthermore, the function of both core cross-linked polymeric micelles on the one hand and nanohydrogels on the other was investigated. Spherical CCPMs (**8**) were formulated with the hydrophobic chemotherapeutic agent paclitaxel (PTX), yielding CCPMs **10** with D_h = 39 nm. Hydrodynamic diameters did not change significantly before and after loading with paclitaxel (Figure 4AI, Table S2). Successful loading and release was confirmed indirectly by *in vitro* cell experiments using human breast cancer cells (TD47 cells). While PTX-loaded CCPMs led to a substantially decreased cell viability, comparable to free paclitaxel, empty CCPMs were non-toxic (Figure 4AII). On the other hand, worm-like nanohydrogels **1** enable complexation of chol-siRNA at N/P ratios of 8 (Figure S10), resulting in nanohydrogels **11** with D_h = 81 nm, once again with unchanged size distributions (Figure S11, Table S2). Additionally, loaded nanohydrogels exhibits near neutral ζ-potentials (surface ζ = 0.4 mV before and ζ = 0.5 mV after loading, Figure 4BI), which is due to effective shielding of the PSar segment. The bio-reversible nature of siRNA complexation was evaluated by agarose gel electrophoresis using extra- and intracellularly relevant glutathione (GSH) concentrations (Figure 4BII). In the absence of GSH and with 10 µM GSH (extracellular), chol-siRNA-loaded nanohydrogels remained stable, whereas siRNA is released at 10 mM GSH (intracellular). The successful loading of respective core-functionalized particles as well as cargo release upon a reductive stimulus portray the last phase of the proposed platform (Figure 1CIII).

In summary, our findings highlight the potential of secondary structure-driven self-assembly to control size and shape of polymeric nanostructures in combination with adjustable core functionality by bio-reversible core cross-linking in a separate, single post-polymerization step. The *S*-ethylsulfonyl protective group for cysteine enables the controlled NCA ring-opening polymerization, which is exploited here for the synthesis of amphiphilic $PSar_n$-*b*-$PCys(SO_2Et)_m$ block copolypept(o)ides. Their self-assembly behavior can be directed by switching the conformation of the polycysteine segment from rod to coil, and tune the polymer association by manipulating the secondary structures. In addition to size and shape control, this approach enables complete decoupling of function from the self-assembly process, since polarity of the micellar core is introduced only after particle formation using dithiol-containing cross-linkers. This novel polypept(o)ide-based nanoparticle platform can be used to generate nanoparticle libraries for various biomedical applications, ranging from nucleic acid delivery (RNAi) over drug delivery to imaging and may help to further elucidate the size and shape dependency of circulation, bio-distribution and cellular responses.

Acknowledgements

The authors would like to Prof. Angelika Kühnle for providing AFM facilities. D.H. would like to acknowledge the support by the “Verband der Chemischen Industrie” (VCI) and the “Max Planck Graduate Center with the Johannes Gutenberg-Universität Mainz” (MPGC). K.K. acknowledges the financial support from graduate school MAINZ and is a recipient of the fellowship through the Excellence Initiative (DFG/GSC 266). O.S acknowledges support by the „Evangelisches Studienwerk e.V. Villigst“.

Keywords: reactive polypept(o)ides • micelles • self-assembly • secondary structure • bio-reversible cross-linking

[1] A. Carlsen, S. Lecommandoux, *Curr. Opin. Colloid Interface Sci.* **2009**, *14*, 329–339.
[2] A. Blanazs, S. P. Armes, A. J. Ryan, *Macromol. Rapid Commun.* **2009**, *30*, 267–277.
[3] H. A. Klok, S. Lecommandoux, *Adv. Mater.* **2001**, *13*, 1217–1229.
[4] C. Cai, J. Lin, Y. Lu, Q. Zhang, L. Wang, *Chem. Soc. Rev.* **2016**, *45*.
[5] Y. Mai, A. Eisenberg, *Chem. Soc. Rev.* **2012**, *41*, 5969–85.
[6] M. Lee, B.-K. Cho, W.-C. Zin, *Chem. Rev.* **2001**, *101*, 3869–3892.
[7] H. M. König, A. F. M. Kilbinger, *Angew. Chemie - Int. Ed.* **2007**, *46*, 8334–8340.
[8] G. Fuks, R. Mayap Talom, F. Gauffre, *Chem. Soc. Rev.* **2011**, *40*, 2475–93.

[9] J. T. Chen, E. L. Thomas, C. K. Ober, G. Mao, *Science* **1996**, *273*, 343–346.
[10] X. Wang, G. Guerin, H. Wang, Y. Wang, I. Manners, M. a Winnik, *Science* **2007**, *317*, 644–647.
[11] J. B. Gilroy, T. Gädt, G. R. Whittell, L. Chabanne, J. M. Mitchels, R. M. Richardson, M. a Winnik, I. Manners, *Nat. Chem.* **2010**, *2*, 566–570.
[12] L. Sun, A. Pitto-Barry, N. Kirby, T. L. Schiller, A. M. Sanchez, M. A. Dyson, J. Sloan, N. R. Wilson, R. K. O'Reilly, A. P. Dove, *Nat. Commun.* **2014**, *5*, 5746.
[13] L. C. Palmer, S. I. Stupp, *Acc. Chem. Res.* **2008**, *41*, 1674–1684.
[14] E. Krieg, M. M. C. Bastings, P. Besenius, B. Rybtchinski, *Chem. Rev.* **2016**, *116*, 2414–2477.
[15] P. A. Korevaar, C. J. Newcomb, E. W. Meijer, S. I. Stupp, *J. Am. Chem. Soc.* **2014**, *136*, 8540–8543.
[16] T. S. Burkoth, T. L. S. Benzinger, D. N. M. Jones, K. Hallenga, S. C. Meredith, D. G. Lynn, *J. Am. Chem. Soc.* **1998**, *120*, 7655–7656.
[17] I. W. Hamley, I. a Ansari, V. Castelletto, H. Nuhn, A. Rösler, H. A. Klok, *Biomacromolecules* **2005**, *6*, 1310–1315.
[18] T. Shimada, S. Lee, F. S. Bates, A. Hotta, M. Tirrell, *J. Phys. Chem. B* **2009**, *113*, 13711–13714.
[19] D. Eckhardt, M. Groenewolt, E. Krause, H. G. Börner, *Chem. Commun.* **2005**, 2814.
[20] Y. Mochida, H. Cabral, Y. Miura, F. Albertini, S. Fukushima, K. Osada, N. Nishiyama, K. Kataoka, *ACS Nano* **2014**, *8*, 6724–6738.
[21] S. Lecommandoux, M.-F. Achard, J. F. Langenwalter, H.-A. Klok, *Macromolecules* **2001**, *34*, 9100–9111.
[22] H.-A. Klok, J. F. Langenwalter, S. Lecommandoux, *Macromolecules* **2000**, *33*, 7819–7826.
[23] H. R. Kricheldorf, *Angew. Chem. Int. Ed. Engl.* **2006**, *45*, 5752–84.
[24] J. Hwang, T. J. Deming, *Biomacromolecules* **2001**, *2*, 17–21.
[25] M. Barz, D. Huesmann, O. Schäfer, T. Reuter, A. Birke, P. Heller, *Thiol-Protected Amino Acid Derivatives And Uses Thereof.*, **2014**, WO2015169908A1.
[26] O. Schäfer, D. Huesmann, M. Barz, *Macromolecules* **2016**, *49*, 8146–8153.
[27] K. Klinker, M. Barz, *Macromol. Rapid Commun.* **2015**, *36*, 1943–1957.
[28] S. L. Perry, L. Leon, K. Q. Hoffmann, M. J. Kade, D. Priftis, K. a. Black, D. Wong, R. a. Klein, C. F. Pierce, K. O. Margossian, et al., *Nat. Commun.* **2015**, *6*, 6052.
[29] O. Schäfer, D. Huesmann, C. Muhl, M. Barz, *Chem. - A Eur. J.* **2016**, *22*, 18085–18091.
[30] R. Holm, K. Klinker, B. Weber, M. Barz, *Macromol. Rapid Commun.* **2015**, *36*, 2083–2091.
[31] T. S. Burkoth, T. L. S. Benzinger, V. Urban, D. G. Lynn, S. C. Meredith, P. Thiyagarajan, *J. Am. Chem. Soc.* **1999**, *121*, 7429–7430.
[32] C. Chothia, *J. Mol. Biol.* **1973**, *75*, 295–302.
[33] T. A. Tockary, K. Osada, Q. Chen, K. MacHitani, A. Dirisala, S. Uchida, T. Nomoto, K. Toh, Y. Matsumoto, K. Itaka, et al., *Macromolecules* **2013**, *46*, 6585–6592.
[34] C. S. Sevier, C. A. Kaiser, *Nat. Rev. Mol. Cell Biol.* **2002**, *3*, 836–847.
[35] S. Matsumoto, R. J. Christie, N. Nishiyama, K. Miyata, A. Ishii, M. Oba, H. Koyama, Y. Yamasaki, K. Kataoka, *Biomacromolecules* **2009**, *10*, 119–127.
[36] J. F. Quinn, M. R. Whittaker, T. P. Davis, *Polym. Chem.* **2017**, *8*, 97–126.
[37] Y. Kakizawa, A. Harada, K. Kataoka, *J. Am. Chem. Soc.* **1999**, *121*, 11247–11248.
[38] J. P. Tam, C. R. Wu, W. Liu, J. W. Zhang, *J. Am. Chem. Soc.* **1991**, *113*, 6657–6662.
[39] M. M. Pakulska, S. Miersch, M. S. Shoichet, *Science* **2016**, *351*, 4750.
[40] C. Lawatscheck, M. Pickhardt, S. Wieczorek, A. Grafmüller, E. Mandelkow, H. G. Börner, *Angew. Chemie Int. Ed.* **2016**, *55*, 8752–8756.

10.1002/anie.201702624

WILEY-VCH

Entry for the Table of Contents (Please choose one layout)

Layout 1:

COMMUNICATION

Worms and spheres: Secondary structure-driven self-assembly allows for the synthesis of spherical and worm-like core cross-linked architectures from the same amphiphilic block copolypept(o)ide. Utilizing bio-reversible disulfide cross-linking, core polarity and function is adjusted independently from particle preparation, offering a versatile biocompatible nanoparticle platform.

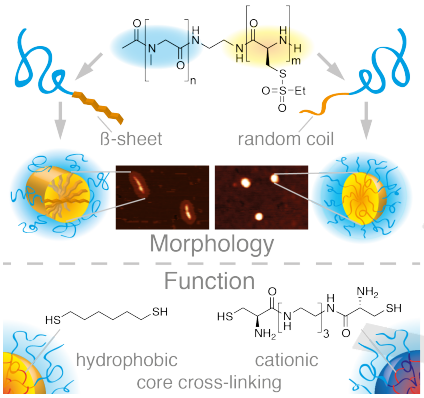

*Kristina Klinker[+], Olga Schäfer[+], David Huesmann, Tobias Bauer, Leon Capelôa, Lydia Braun, Natascha Stergiou, Meike Schinnerer, Anjaneyulu Dirisala, Kanjiro Miyata, Kensuke Osada, Horacio Cabral, Kazunori Kataoka, Matthias Barz**

Page No. – Page No.

Secondary Structure-Driven Self-Assembly of Reactive Polypept(o)ides: Controlling Size, Shape and Function of Core Cross-Linked Nanostructures